Model-based Investigation of the Coupling between the Cell Cycle and the Circadian Clock in Mouse Embryonic Fibroblasts[☆]

Pauline Traynard[a], Céline Feillet[b], Sylvain Soliman[a], Franck Delaunay[b], François Fages[a]

[a] *Inria, Lifeware Group, Saclay, France*
[b] *CNRS, INSERM, Institut de biologie Valrose, Université Nice Sophia Antipolis, France*

Abstract

Experimental observations have put in evidence autonomous self-sustained circadian oscillators in most mammalian cells, and proved the existence of molecular links between the circadian clock and the cell cycle. Some mathematical models have also been built to assess conditions of control of the cell cycle by the circadian clock. However, recent studies in individual NIH3T3 fibroblasts have shown an unexpected acceleration of the circadian clock together with the cell cycle when the milieu is enriched in FBS, the absence of such acceleration in confluent cells, and the absence of any period doubling phenomena. In order to explain these observations, we study a possible entrainment of the circadian clock by the cell cycle through a regulation of clock genes around the mitosis phase. We develop a computational model and a formal specification of the observed behavior to investigate the conditions of entrainment in period and phase. We show that either the selective inhibition of *Bmal1* transcription, or the selective activation of *RevErb-α* at the end of the mitosis phase, allow us to fit the experimental data, while a uniform inhibition of transcription during mitosis seems incompatible with the phase data. We conclude on some further

[☆] This article is the extended revision of a preliminary communication published in [1].

Email addresses: Pauline.Traynard@inria.fr (Pauline Traynard), Celine.Feillet@unice.fr (Céline Feillet), Sylvain.Soliman@inria.fr (Sylvain Soliman), Franck.Delaunay@unice.fr (Franck Delaunay), Francois.Fages@inria.fr (François Fages)

predictions of the model.

Keywords: Quantitative biology, Circadian clock, Cell Cycle, Model coupling, Data fitting, Oscillations, Formal methods, Model Checking

---

1. Introduction

Most organisms, from bacteria to plants and animals, have a circadian clock present in each cell, generally in the form of a self-sustained genetic oscillator entrained by the day/night cycle through various mechanisms. This circadian clock has many effects on cell signaling and metabolism [2]. Experimental results have also shown a regulation of the cell division cycle by the circadian clock [3, 4, 5], with possible applications to cancer chronotherapies [6, 7]. Molecular links between these two cycles have been exhibited to explain this regulation. In particular the regulation of Wee1, an inhibitor of the G2/M transition, by the clock genes has been proposed to explain the circadian gating of mitosis during the liver regeneration process [3] and the 48h period doubling phenomena of the cell cycle [8]. Other similar molecular links going in the same direction, through p21 [9] and Chk1 and Chk2 [5, 10], have been shown in different cells in the literature. A few models have also been developed to further investigate those hypotheses, by coupling a model of the cell cycle with a model of the circadian clock through those direct molecular links, and analyzing the conditions of entrainment in period [11, 12].

However, in mouse embryonic fibroblasts NIH3T3, several studies using large-scale time-lapse microscopy to monitor circadian gene expression and cell division events in real time and in individual cells during several days have unveiled unexpected behaviours, hinting that the relationship might be more complex. Nagoshi et al. [8], have first shown that circadian gene expression in fibroblasts continues during mitosis, but with a consistent pattern in circadian period variation relatively to the circadian phase at division, leading them to hypothesize that mitosis elicits phase shifts in circadian cycles. A more recent study of Bieler et al. [13] relating the same experiments on dividing fibroblasts

found the two oscillators synchronized in 1:1 mode-locking leading the authors to hypothesize a predominant influence of the cell cycle on the circadian clock in NIH3T3 cells. This is in agreement with another detailed experimental study of Feillet et al. [14] which found several different synchronization states in NIH3T3 fibroblasts in different conditions of culture. In particular, it was observed in [14] that enriching the milieu with Foetal Bovine Serum (FBS) not only accelerates the cell division cycle but also the circadian clock. For cells cultured in 10% FBS, both distributions of the cell cycle length and the circadian clock are centered around 22h. For cells cultured in 15 % FBS, both the cell cycle and the circadian clock accelerate, with period distributions centered around 19h. However, when cells reach confluence and stop dividing, the circadian clock slows down and the period distribution is then centered around 24h. None of the currently available models coupling the cell cycle and the circadian clock can explain these observations since they are based on an unidirectional influence of the circadian clock on the cell cycle [11, 12].

In this paper, in order to explain these observations, we study the reverse influence of the cell cycle on the circadian clock, using computational modeling tools. We develop a mathematical model of the influence of the cell cycle on the circadian clock through the differential regulation of clock genes around the mitosis phase, and investigate the conditions in which the cycles are entrained in period and phase as observed in [14]. For this, we use the circadian clock model of Relogio et al. [15] which has been carefully fitted to phase data on suprachiasmatic cells, and a simple model of the cell cycle by Qu et al. [16] which focuses on the mitosis phase. In [1], we have already shown that the uniform inhibition of transcription during mitosis, as observed in eukaryotes [17], could explain the acceleration of the circadian clock in non-confluent cells when the concentration of FBS increases. In particular, our model could reproduce the same periods for the cell cycle and the circadian clock observed in [14] for different levels of FBS, modeled by different values for the synthesis parameters of the cell cycle model. However this model displayed an incorrect time delay between the cell division and the peak of Reverb-α, which seemed impossible to

fix under the hypothesis of a uniform inhibition of transcription during mitosis. Here, we show that these difficulties can be resolved, using a different hypothesis of selective regulation of one clock gene triggered at the end of the M phase, either the inhibition of *Bmal1*, or the activation of *Reverb-α*. Indeed, our coupled model under one of these hypotheses is able to reproduce the measures on periods and phases made by Feillet et al. [14] in individual unperturbed fibroblasts. Furthermore we argue that the complex behaviors observed with high variability after a treatment by Dexamethasone to synchronize cellular clocks, modeled by the induction of a high level of *Per* and the inhibition of the other clock core genes, can be explained by the perturbation of the clock after this treatment. Indeed, our model shows that the stabilization time after that pulse appears to be greater than the time horizon of 72h used in those experiments.

This computational model has been built using the BIOCHAM modeling software [18] for

1. importing and exporting models in SBML, and modeling the molecular interactions of the coupling of the models,
2. specifying the observed behavior in quantitative temporal logic using pattern formulae for periods and phases [19, 20],
3. searching parameter values [21] and measuring robustness and parameter sensitivity indices [22] with respect to the temporal logic specification of the dynamical behavior[1].

2. Experimental Data and their Formal Specification in Temporal Logic

2.1. Experimental Observations and Measurements

In this section we explain the single cell experiments and analyses performed in [14] and the conclusions drawn by the authors. The reported experiments have been done using time lapse videomicroscopy and cell tracking using various

[1]The models and the specification used in this paper are available on `http://lifeware.inria.fr/wiki/software/biosystems16`.

fluorescent reporters for the cell cycle and the circadian clock observed during 72 hours in proliferating NIH3T3 mouse fibroblasts.

The NIH3T3 embryonic mouse fibroblasts were modified to include three fluorescent markers of the circadian clock and the cell cycle: the RevErb-α::Venus clock gene reporter for measuring the expression of the circadian protein RevErb-α, and the Fluorescence Ubiquitination Cell Cycle Indicators (FUCCI), Cdt1 and Geminin, two cell cycle proteins which accumulate during the G1 and S/G2/M phases respectively, for measuring the cell cycle phases.

The cells were left to proliferate in regular medium supplemented with different concentrations of FBS (10% and 15%). Long-term recording was performed in constant conditions with one image taken every 15 minutes during 72 hours. The lengths of the cell cycles were measured as the time interval between two consecutive cell divisions.

The expression traces of RevErb-α proteins were detrended and smoothed. Spectrum resampling was used to estimate the clock period. Cells with less than two RevErb-α peaks within their lifetime, a period length outside the interval between 5 hours and 50 hours or a relative absolute error (RAE) bigger than 0.25 (showing a confidence interval wider than twice the estimated period) were classified as non-rhythmic and discarded, assuming that they do not have a functioning clock. Finally, the delay between mitosis and the next clock marker peak was measured. It revealed that RevErb-α-Venus peaked about 7 h after cell division in all conditions, quite consistently with the delay of 5h for Reverb-α without Venus observed in [23] and [13].

The quantitative data on the periods of the cell cycle and the circadian clock and the phase between them are summarised in Table 1 [14]. Surprisingly, increasing FBS from 10% to 15%, not only decreases the mean period of the cell cycle from 21.9h to 19.4h, but also the clock period from 21.3h to 18.6h, i.e. to essentially the same period. This shows that both oscillators remain unexpectedly in 1:1 mode locking. While the speedup of the cell cycle can be directly attributed to the growth factors in increasing concentration of FBS, it can not account for the speedup of the clock the same way, since confluent

cells keep a 24-hours period for the circadian clock independently of the FBS concentration.

Medium	Clock period	Division period	Delay
FBS 10%	21.9h ± 1.1h	21.3h ± 1.3h	8.6h
FBS 15%	19.4h ± 0.5h	18.6h ± 0.6h	7.1h

Table 1: Estimated periods of the circadian molecular clock and the cell division cycle measured in [14] in fibroblast cells without treatment by Dexamethasone, for two concentrations of FBS. The time delay is between the cell division time and the next peak of RevErb-α.

2.2. Experimental Observations after Treatment by Dexamethasone

Furthermore, a series of experiments were done with a pulse of dexamethasone (Dex) before recording. This glucocorticoid agonist is known to exert a resetting/synchronizing effect on the circadian molecular clocks in cultured cells through the induction of *Per1*. In that case the cells were incubated for 2 hours in the same medium supplemented with Dex, just before returning to a Dex-free medium for the recording.

In that case, the results are more complex. As summarized in Table 2 which contains values from [14], the cells in 10% FBS show an increased clock period and a low cell cycle period, with an overall ratio of 5:4. In 20% FBS the cell lineages are dominated by two groups. The first group shows close periods, i.e. a 1:1 mode-locking similarly to the experiments without dexamethasone. The second group shows a high clock period and a fast cell cycle, with an overall ratio close to 3:2 between the clock and cell cycle, explaining the three-peaks distribution of the circadian phase at division, as already observed by Nagoshi et al.[8] ten years before. It has to be noted that the 20% FBS dexamethasone-synchronized experiment was repeated with similar results available in the Supplementary Information of [14], although the distribution of the period ratios for the second group is wider in the interval $[1.2, 2]$.

In [14], the authors suggest that these observations might be interpreted by the existence of distinct oscillatory stable states coexisting in the cell populations, in particular with 5:4 and 1:1 phase-locking modes for the condition

Medium	Clock period	Division period	Delay
FBS 10%	24.2h ± 0.5h	20.1h ± 0.94h	10.7h
FBS 20%	21.25h ±0.36h	19.5h ±0.42h	8.3h
	29h±1.05h	16.05h±0.48h	6h/12h/22h

Table 2: Estimated periods of the circadian molecular clock and the cell division cycle measured in [14] in fibroblast cells after treatment by Dexamethasone, for two concentrations of FBS. The time delay is between the cell division and the next peak of RevErb-α. The experiment done with 20% FBS have been clustered by the authors of [14] in two groups with different periods.

10% FBS, and 3:2 and 1:1 phase-locking modes for the condition 20% FBS, and that the dexamethasone could knock the state out of the 1:1 mode toward other attractors. A mechanistic explanation remains to be found to support this interpretation.

2.3. Formal Specification of Oscillation Properties in Quantitative Temporal Logic

For the analysis of the dynamical behavior of this complex system, we shall make use of a temporal logic language which allows us to formalize the oscillatory properties of the system, without over-specifying them by providing a curve to fit. It allows us to combine qualitative properties of oscillations and quantitative properties on the shapes of the traces such as distances between peaks or peak amplitudes. This is useful to capture the periods on both experimental and simulated traces, even when the traces are irregular and noisy. We use formal constraints on the amplitudes and regularity of the peaks to filter out ambiguous traces, keeping only sustained oscillations even with small irregularities, as it is the case for example in Fig. 9.

More precisely, we use the temporal logic formula patterns described in [19, 20] and implemented in our modeling software BIOCHAM [18] to specify the constraints about the successive peaks of concentrations between either the same molecular species (period constraints) or different molecular species (phase constraints). BIOCHAM then provides commands for automatically

- extracting periods and phases from either simulation or experimental numerical data time series [24],

- searching the space of the unknown parameters of the model for satisfying period and phase constraints [21],
- measuring parameter sensivity indices and robustness with respect to period and phase constrainst [22].

For instance, the following command computes the validity domain for a formula pattern used to extract the period of MPF for the cell cycle and RevErb-α for the circadian clock (see Section 3) in a trace, and their relative phase:

```
validity_domain(
Exists([e1,e2,e3],
 periodErrors([RevErb_nucl],[periodselect,e1,e2,e3],100)
 & e1<2 & e2<2 & e3<2))
& period([MPF],[periodMPF])
& phase([MPF,RevErb_nucl],[phase])).
```

The result for the simulation trace obtained with *kdie=0.25* and displayed in Fig. 7 is

```
periodselect = 17.7763, periodMPF = 18.066, phase = 2.09856
```

The period constraint on the oscillations of RevErb-α is expressed by the temporal logic function *periodErrors*, whose validity domain provides the mean of the last two RevErb-α peak-to-peak intervals in the variable *periodselect*, along with several variables characterizing irregularity features of the trace, after a transient time of 100h to avoid irregularities caused by the initial state: *e1* for the irregularities in distances between peaks (it denotes the maximum difference between two intervals), *e2* for the irregularities in the amplitudes of the peaks (it quantifies the differences between the amplitudes of the peaks), and *e3* being a non-null error if the concentration amplitude is too small (below 0.1). Setting thresholds on these variables ensures that irregular traces are filtered out. The operator *Exists* projects the resulting validity domain on the single dimension for *periodselect*. Since the trace of MPF shows sustained and regular oscillations in all simulations, the simple function *period* is used to extract the mean of the last two peak-to-peak intervals. Moreover, the function *phase* captures the mean of the last two time intervals between MPF and RevErb-α peaks.

On the other hand, it is worth remarking that for the purpose of exploring the parameter search, irregular traces should not be filtered out in order to orient the search algorithm in a promising direction, when oscillations begins to appear for instance. This can be specified in temporal logic with the following constraint:

```
add_search_condition(
periodErrors([RevErb_nucl],[period,e1,e2,e3],100) &
Exists([phase],
  phase([MPF,RevErb_nucl],[phase])
  & phase>minphase & phase<maxphase)
,[period,e1,e2,e3,minphase,maxphase],[21.3,0,0,0,3,5.5],
300,[(kdie,kdie21)]).
```

For each set of parameter values tested during the calibration procedure, this command computes the euclidian distance between the values found for *[period,e1,e2,e3,minphase,maxphase]* and the objectives *[21.3,0,0,0,3,5.5]*, in the condition *kdie=kdie21* and a simulation time of 300h. This distance is used as a score for the satisfaction of the temporal logic formula on the trace. The additional variables *minphase* and *maxphase* allow to score the distance from the phase to the objective interval [3,5.5], enabling some flexibility in the searched value for the phase. For instance, the best set of parameters found as a solution after the calibration procedure detailed in 4.2 has the score 0.54 for this specification.

The temporal logic language allows us to combine the variables, for example with the difference between the periods of the cell cycle and the circadian clock, which can then be used to score the entrainment in period of the circadian clock by the cell cycle. This is illustrated by the following command:

```
satisfaction_degree(
Exists([p1,p2],Exists([e1,e2,e3],
        periodErrors([RevErb_nucl],[p1,e1,e2,e3],100)
        & e1<3 & e2<3 & e3<3)
& period([MPF],[p2]) & diff=p2-p1),
[diff],[0],300).
```

This specification is used to compute the satisfaction degrees displayed in Fig. 6. Each value scores the difference between the two periods with a value between 0 (infinite difference) to 1 (null difference, perfect entrainment).

3. Cell Cycle and Circadian Clock Models

3.1. Model of the Cell Cycle

The cell cycle of mammalian cells is composed of five phases: the quiescent phase G0 where cells can stay without dividing, the growing phase G1 for entering the cell cycle, the DNA replication phase S, the gap phase G2, and the chromosome segregation and mitosis phase M phase. Each phase is characterized by a particular protein of the cyclin family, which forms a complex with a cyclin-dependent-kinase (CDK) and determines the activity of the phase. The mouse embryonic fibroblast cells considered in this paper are quickly dividing cells. However, those cells also reach confluence and the G0 quiescent phase when they have no more space to divide, i.e. G0 by contact inhibition.

For our purpose of investigating the hypothesis of a regulation of some clock genes around mitosis, it is sufficient to use a cell cycle model focusing on the mitosis phase. We use a model proposed by Qu et al. [16] in which the cell cycle is divided in two different phases: the G1/S/G2 phase and the M phase. Of course, more detailed models distinguishing the four phases of the cell cycle exist, e.g. [11], making possible to represent various regulations of the cell cycle by the circadian clock genes, for instance through p21 and c-Myc on G1, and Wee1 on the G2/M transition. However, since the consequences of those regulations have not been observed in the experimental data considered in this paper, those extra details are irrelevant and we concentrate on the reverse effect of the cell cycle on the circadian clock by the regulation of clock genes around mitosis, for which the simpler two phase model of Qu et al. [16] is sufficient.

In this model,the M phase is triggered by the complex Cdk1/Cyclin-B. This complex appears in two forms, an active form called MPF (M-phase Promoting Factor) and a phosphorylated, inactive form called preMPF. MPF is phosphorylated and inactivated by the kinase Wee1, and dephosphorylated and activated by the phosphatase Cdc25. Both the kinase and phosphatase activities are themselves regulated by MPF, respectively inactivated and activated by the complex, as depicted in Figure 1.

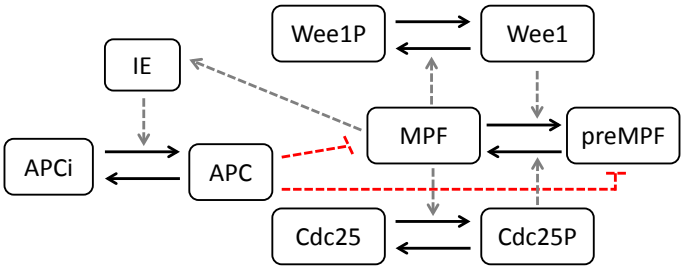

Figure 1: Schema of the cell cycle model of Qu et al. [16]. Solid arrows represent biochemical reactions while dashed arrows denote enzyme catalysis. Red arrows denote an inhibition through activation of the degradation.

In this model, we assessed the effect of the different reaction rate constants on the period of the cell cycle by sensitivity analysis. We found that two parameters are able to change widely the range of the cell cycle period without changing significantly the strength of the coupling: *kdie*, the degradation rate constant of the intermediary enzyme involved in the negative feedback loop between MPF and the proteasome APC, particularly important in G1/S, and *kampf*, the activation rate constant of MPF by Cdc25p, which plays a role in G2/M. In the supplementary material of [14], both the phases G1 and S/G2/M seem to be shortened in enriched FBS. Therefore there is no reason to prefer to choose *kdie* (active in G1) or *kampf* (active in G2/M) to modulate the cell cycle period and we arbitrariily choose to choose *kdie* as varying parameter affected by FBS. Similar results are obtained with *kampf*.

A simple parameter search gives the following values for *kdie*: 0.147 for a cell division period of 21.3 hours (corresponding to 10% FBS), and 0.23 for a period of 18.6 hours (15% FBS).

3.2. Model of the Circadian Clock

In many organisms, spontaneous gene expression oscillations with a period close to 24 hours have been observed. A biochemical clock present in each cell is responsible for maintaining these oscillations at this period. Indeed, it has been shown [25] that in absence of synchronisation by a central clock, autonomous circadian oscillators are maintained in peripheral tissues with the

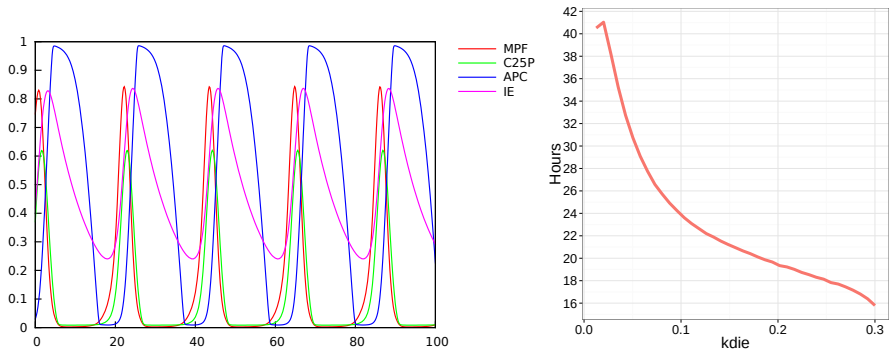

Figure 2: **Left**: Simulation of the cell division cycle model of Qu et al. **Right**: Period of the cell division cycle (measured as the distance between successive peaks of MPF) as a function of the parameter *kdie* for MPF activation by Cdc25p in the model of Qu et al.

same period, although they are progressively desynchronized. This has been confirmed in cultured NIH3T3 cells first in [8] and then in [13] and [14]. In each of those studies, confluent fibroblasts have a circadian clock period close to 24h regardless of the medium concentration.

In this paper we use the circadian clock model of Relogio et al. [15] which has been fitted on mouse suprachiasmatic neurons with precise data on the amplitude and phases of the different components. This model is composed of 20 species, 71 parameters, and all the feedback loops described above. Two major transcription factors, Clock and Bmal1 heterodimerize and activate the transcription of the period (*Per1* and *Per2*), cryptochrome (*Cry1* and *Cry2*), *RevErb-*α and *Ror* clock genes. The newly form Per and Cry proteins associate and inhibit their own expression and that of the RevErb-α and Ror proteins through direct inhibition of the Clock/Bmal1 transcriptional activity. Further, the antagonistic RevErb-α and Ror transcription factors regulate the rhythmic transcription of *Bmal1* and *Clock*. These interlocked feedback loops generate robust 24h self-sustained oscillations that in turn control the expression of a large set of downstream clock-controlled genes. A simulation trace of this model is shown in Figure 3.

This model has been precisely fitted to the observations made on the clock gene reporters in mouse suprachiasmatic nucleus neurons, however without data

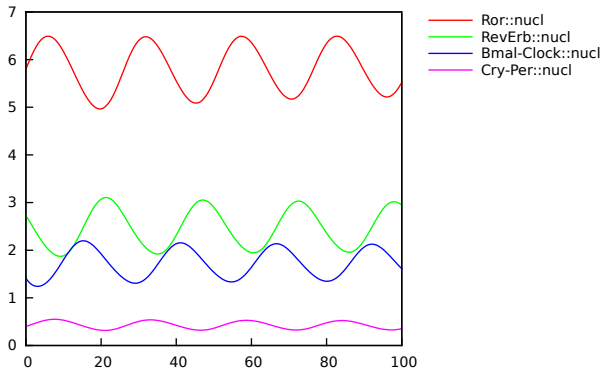

Figure 3: Simulation trace of the Circadian Clock model of Relogio et al. over a time horizon of 100h.

about cell divisions. On the other hand, in the data of Feillet et al.[14], RevErb-α is the only marker on the circadian clock and no comparison is thus possible with the other clock genes.

4. Coupled Model

4.1. Hypothesis of a Selective Regulation of Clock Gene Transcription triggered by Mitosis

In this paper, we investigate the hypothesis that a differential inhibition/activation of some clock genes around the mitosis phase could explain the observations made and reproduce consistent values for the period of the circadian clock and the delay between the divisions and RevErb-α-Venus peaks for the different values of FBS.

To assess this hypothesis, we model the inhibition or activation of clock genes transcription with five multiplicative coefficients I_i ($i \in [1..5]$), associated to the synthesis rate parameters of the model of Relogio et al. [15] for each of the five clock genes. Each coefficient takes the value 1, except during a window starting at mitosis where its value is changed with an event, triggered by the decrease of MPF. Another event is triggered at the end of the regulation window to reset the coefficient. During this window, whose length is defined by a parameter *duration*, the coefficient for the circadian core gene i takes the value of

the dimensionless parameter $coefsynth_i$, that defines the inhibition/activation strength of this clock gene. This value is included in the interval $[0, 3]$, where 0 denotes a full inhibition (i.e., strong coupling), 1 marks no effect of the mitosis on the synthesis (no coupling), and more than 1 induces some activation (coupling again). The value of the regulation *duration* parameter is also considered in the interval $[0, 3]$ hours.

Our coupled model of the cell cycle and the circadian clock thus uses six parameters: the regulation strengths of the clock genes ($coefsynth_i$ ($i \in [1..5]$), and the duration of the regulation:

```
parameter(duration,2).
parameter(endMitosis,0).

For each clock gene i:
parameter(I_i,1).
parameter(coefsynth_i,0).

add_event([MPF]<0.5,endMitosis,Time+duration).
add_event([MPF]<0.5, I_i, coefsynth_i).

add_event(Time>=endMitosis, I_i, 1).
```

It is worth noting that this way of coupling the models enforces the fact that for quiescent cells, whatever the FBS concentration is, the transcription rate will be unaffected by mitosis and therefore the clock will keep a period of 24h, as observed in the experiments.

4.2. Search of Coupling Parameter Values

We use the parameter search procedure of Biocham to find the sets of values for the coupling parameters that reproduces the entrainment in period and phase observed in the data. Using the specification detailed in the section 2.3, we define a multi-condition objective: in the conditions $kdie$=0.1, $kdie$=0.147, $kdie$=0.18 and $kdie$=0.23, the period of the circadian clock must be equal to the period of the cell cycle: respectively 24h, 21.3h, 20h and 18.6h. In each condition, the delay between MPF and RevErb-α peaks must be between 6.5h and 8.6h.

Parameters	**First set**	**Second set**
Synthesis coefficient for *Per*	0.66	2.40
Synthesis coefficient for *Cry*	2.30	0.67
Synthesis coefficient for *RevErb-α*	1.04	1.92
Synthesis coefficient for *Ror*	2.1	1.51
Synthesis coefficient for *Bmal1*	0	0.78
Duration	2.97h	2.81h

Table 3: Two sets of parameter values found by the calibration procedure. The first set was found with null initial values for all synthesis coefficients, while the second was found with initial values of 1.

Two solutions are shown in Table 3. If the parameter search starts from a full inhibition triggered by mitosis for all clock genes, corresponding to initial values of 0 for all synthesis coefficients, the best result found after 260 iterations on a population of 95 sets of parameters gives the first set of parameters reported in Table 3. This solution corresponds to a full inhibition found for the transcription of *Bmal1*, and a smaller inhibition for the transcription of *Per*. The transcription of *Cry* and *Ror* are activated while the transcription of *RevErb-α* is mostly unaffected.

However, when the initial values are 1 for all synthesis coefficients, corresponding to no inhibition during mitosis, the second set is the best result found after 55 iterations on a population of 95 sets of parameters. Here, the transcriptions of *Bmal1* and *Cry* are weakly inhibited, while the transcription of the other clock genes are activated.

The simulation of the model with any of these two sets of parameters shows a delay between the starting time of the mitosis effect and the circadian clock consistent with the experimental data (close to 7h for the first set, and between 7 and 8.5h for the second one). However the first solution yields more consistent results for the time between mitosis and the next RevErb-α peak in cells where the cell cycle is slow, as observed in [8] and [13] and explained below in Section 5.1. For this reason, we focus on this solution in this section. The second solution found is analysed as an alternative hypothesis in Section 5.1.

The parameter search procedure of Biocham returns numerical values for

all coupling parameters, however we must verify which parameter values are necessary for the correct entrainment, and which parameters have no impact on the satisfaction of the specification of the behavior. To this end, we compute the response curves for the period of the circadian clock and the delay between mitosis and the next RevErb-α peak for each calibration parameter, in the condition where the cell cycle has a period of 21h. The results are shown in Fig. 4.

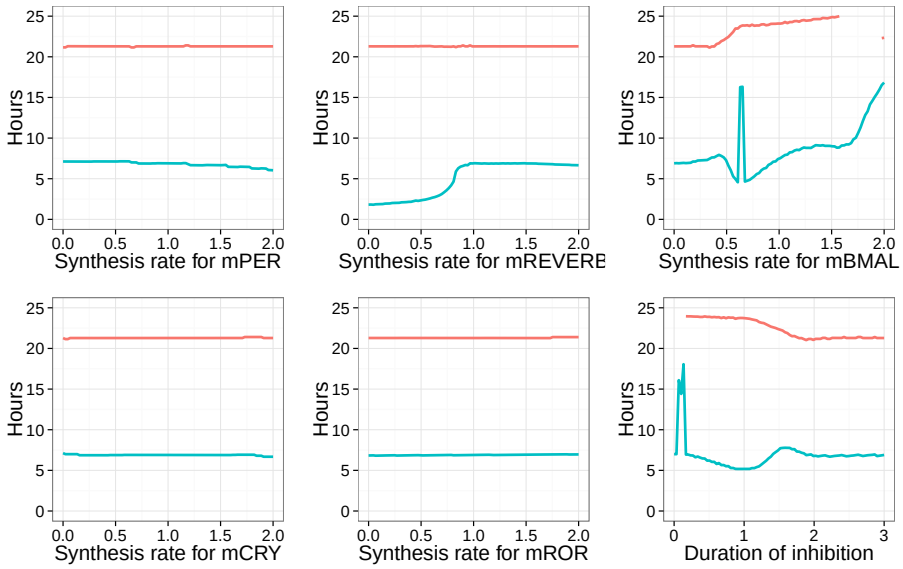

Figure 4: Period of the circadian clock (red) and time delay between MPF and RevErb-α peaks (blue) in the coupled model calibrated with the first set of parameters, and when the cell cycle has a period of 21h. The peaks on the blue curves on the right figures characterize irregular oscillating traces (due to a partial entrainment in period).

These simulation results reveal that the entrainment in period and phase of the circadian clock depends only on the effect of the mitosis on *Bmal1* and *RevErb-α*, and the duration of this effect. Varying the synthesis coefficients during mitosis for *Per*, *Cry* or *Ror* has no significant effect on the entrainment.

The inhibition of *Bmal1* is crucial for the entrainment in period. More specifically, the clock is entrained to the cell cycle period of 21h if the coefficient multiplied to the synthesis rate of *Bmal1* is at most 0.4, and the inhibition

lasts at least 2h. Interestingly, the inhibition on *RevErb-α* has no effect on the period of the circadian clock, although it has an effect on the circadian phase at division. With a low or absent inhibition of *RevErb-α* (corresponding to a coefficient higher than 0.8), the time delay between divisions and RevErb-α peaks is consistent with the data, with RevErb-α peaks occuring 7h after division. Adding an inhibition of *RevErb-α* triggered by mitosis would conserve the entrainment of the circadian period, but the RevErb-α peaks occur just after mitosis.

These new simulations point toward a new hypothesis of a selective inhibition of the circadian clock gene *Bmal1* triggered by mitosis. In the rest of the paper, the coupling parameters are simplified to consider a single inhibition of *Bmal1* (corresponding to a coefficient equal to 0), and no effect on the other clock genes.

4.3. Simulation Results for the Selective Inhibition of Bmal1 at the end of Mitosis

kdie	FBS %	Circadian clock period (h)	Cell division period (h)	Phases (h)
0.077	5?	26.09	26.10	23.2
0.147	10	21.28	21.28	6.8
0.229	15	17.99	18.60	6.3

Table 4: Periods and time delays reproduced by the coupled model with different values of *kdie* for modeling the different culture conditions (the correspondance with 5% FBS is speculative since no experiment was done in this condition). The delays are the time observed by simulation between the peaks of concentration of MPF and RevErb-α.

Table 4 shows the periods of the circadian clock and the cell division cycle and the delay between the starting time of the inhibition of *Bmal1*, when the peak of MPF overtakes the threshold 0.5, and the following peak of RevErb-α in our model with different values of *kdie* corresponding to the different culture conditions. In all cases, the cell division manages to entrain the circadian clock (that has a free period around 24h) to its period, simply through this mechanism of selective transcription inhibition, as depicted in Fig. 5. These simulation results reproduce quite well the data of Table 1 when there is no treatment

by Dex. Note that our model can also have a cell division time higher than 24h, for instance with *kdie*=0.077 which might correspond to a concentration of FBS around 5%. In that case the model predicts that the cell cycle will still entrain the circadian clock, lowering its period. Moreover, RevErb-α peaks are predicted to occur slightly before cell divisions in this condition, with a delay of 23.2h between the inhibition of *Bmal1* and the following peak of RevErb-α.

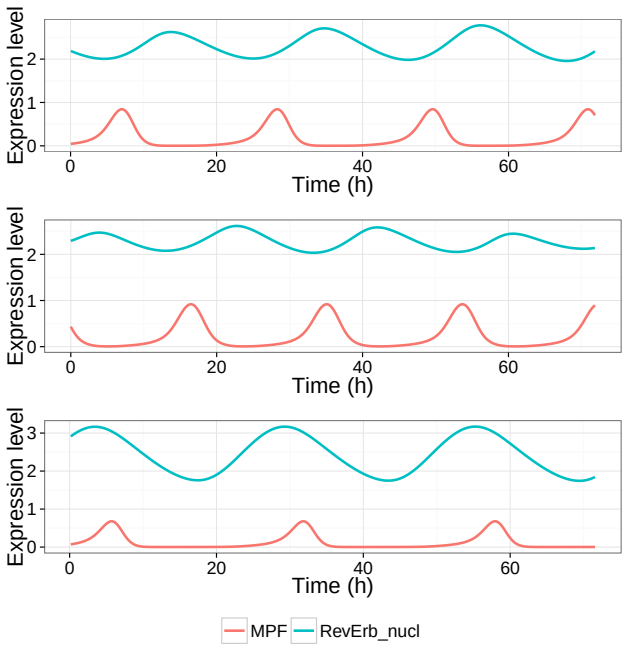

Figure 5: Simulation of the model with the inhibition of the transcription of *Bmal1* triggered by mitosis, during 72h. Top: the cell cycle has a period of 21.3h. Middle: the cell cycle has a period of 20.1h. Bottom: : the cell cycle has a period of 26h.

As shown in the right panel of Fig. 2, it is possible to simulate the experimental milieu enrichment with 10 or 15% FBS by varying the parameter *kdie* of the cell cycle model to obtain the same values for the period of the cell division cycle.

The landscape in Fig. 6 is computed to assess the role of the inhibition or activation duration. It shows the variation of the difference between the periods of RevErb-α for the circadian clock and *MPF* for the cell cycle when the two

parameters *kdie* and *duration* vary. The value of each period is captured with a temporal logic specification as seen in the subsection 2.3. The result for the inhibition of *Bmal1* is shown in Fig. 6, and is very similar to the result in the case of an activation of *RevErb*-α.

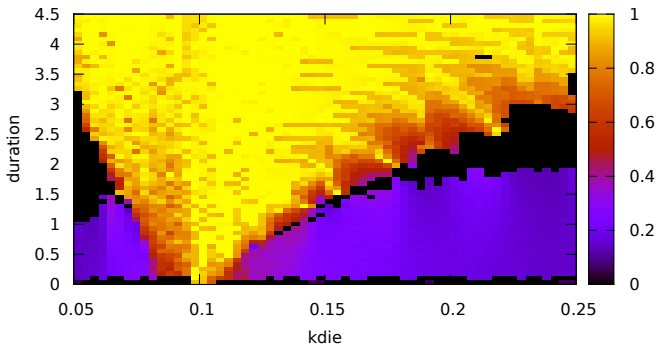

Figure 6: Absolute difference between the periods of the circadian clock and the cell cycle, as a function of *kdie* for varying the cell cycle period, *duration*, the duration of the inhibition of *Bmal1* transcription triggered by mitosis. The landscape is computed as the satisfaction degree of the third formula detailed in 2.3. The color translates the distance from the value found for the period difference *diff* to the objective 0. Full satisfaction in yellow indicates equal periods for MPF and RevErb-α, while the other colours indicate the absolute difference. Black indicates an absence of result for the specification, meaning that the regularity constraints set on the trace of RevErb-α with the function *periodErrors* were not met.

Three domains can be distinguished in this parameter space: in the domain in yellow, the circadian clock is entrained to the same period as the cell cycle. This domain of entrainment is wider for a long duration of inhibition. For a short duration, the circadian clock can only be entrained by the cell cycle if the entraining period is close to 24h. In the purple domain at the bottom (for a low value of *duration*), the difference between the two periods is high because the clock is not entrained, hence it keeps its period constant and close to 24h. Finally, these two domains are separated by a black domain where the clock oscillations are partially entrained and become irregular.

One can notice that the longer the inhibition of *Bmal1*, the wider the range of values of *kdie* over which the circadian clock can be entrained. In particular,

the clock can be entrained by the cell cycle when $kdie = 0.23$, corresponding to the smallest period (18h) reported in the data, if the duration of the inhibition is at least 3h.

The entrainment both in period and phase with an inhibiting effect during 3h is visualized in Fig. 7. It shows the response curve for the periods of the cell cycle and the circadian clock, and the time delay between the peaks of MPF and RevErb-α in the simulations when the parameter *kdie* varies.

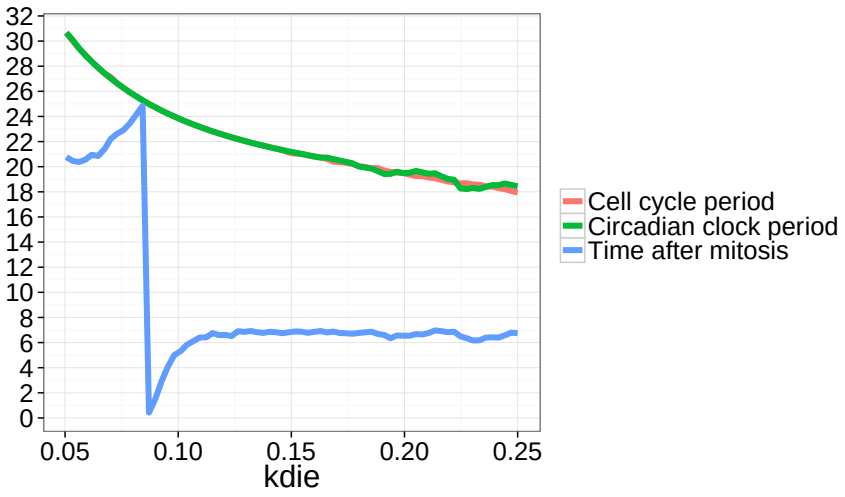

Figure 7: Entrainment in period and phase of the circadian clock when the period of the cell cycle varies with the parameter *kdie*, with the inhibition of *Bmal1* triggered by mitosis. The blue curve depicts the time delay between peaks of MPF and RevErb-α in the simulations.

4.4. Predictions on the phases in the clock

Data on the phases between clock components in proliferating cells are sparse. The model allows us to investigate whether the coupling from the cell cycle affects the phases between clock mRNAs and proteins. The following in-silico experiment is performed to this end: in the coupled model with a fast cell cycle (21h), the strength of the inhibition of *Bmal1* is changed in a set of simulations and the phases between clock components are captured in each simulation, normalised by the clock period, as shown in Fig. 8.

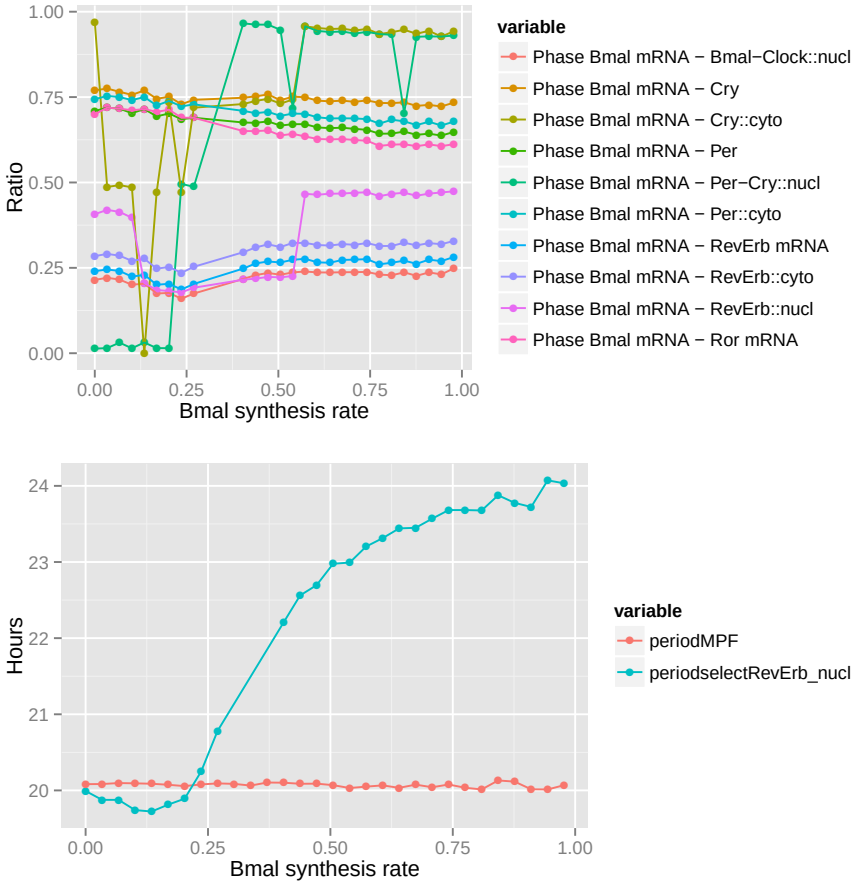

Figure 8: Circadian clock phases in the coupled model when the cell cycle has a period of 21h and the inhibition of *Bmal1* varies.

The simulations reveal that in the entrained condition (when the synthesis rate of *Bmal1* is inhibited with a coefficient smaller than 0.2), the phases between clock components are not deeply impacted by the periodic inhibition on *Bmal1* resulting from the coupling with the cell cycle, compared to their values in the free clock (when the synthesis rate of *Bmal1* is inhibited with a coefficient higher close to 1). However, the phase between *Bmal1* and *RevErb-α* mRNAs shows a small advance, that impacts similarly the phases between Bmal1 and RevErb-α in the cytoplasm and in the nucleus. Notably, the other clock genes and proteins targeted by Bmal1 exhibit a phase delay when the synthesis of *Bmal1* is inhibited during mitosis.

4.5. Comparison to Experimental Data after Treatment by Dexamethasone

In order to take into account the experiments with Dexamethasone, the model can be extended with an event, lasting for two hours, and inducing *Per* mRNA while inhibiting the other clock genes.

Fig. 9 shows that in our models, regardless of the milieu (i.e. of the value of *kdie*), the Dex pulse results in a perturbation of the clock and then returns to the observed entrainment.

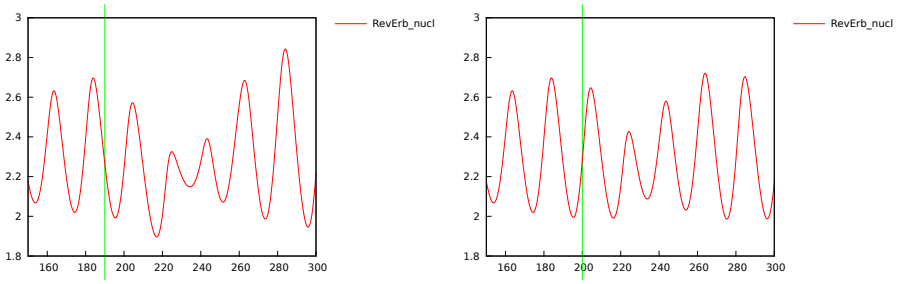

Figure 9: Effect of a Dexamethasone pulse on the entrainment resulting from the periodic inhibition of *Bmal1* synthesis by the cell cycle. The pulse alters the clock before returning to the previously observed entrainment regime. In the left panel the pulse is from time 190 to 192 while on the right it is from 200 to 202. The left panel's peak-to-peak distance is in the $[18.2, 21.2]$ interval, while the right one remains in the $[19.31, 20.7]$ interval. This might correspond to the two groups observed in [14]. The time to recover normal entrainment varies but is often larger than 72h.

These simulations point us to the possibility that the noisy data reported in Table 1 after the Dex pulse might simply be due to the various cellular states

in which the pulse happened and to the time necessary for the cells to recover their clock entrainment, rather than to two different oscillatory attractors of the system.

A pulse at time 200h disrupted only slightly our clock, leading to mostly remaining in mode-locking 1:1, whereas advancing that same pulse by 10h (corresponding to giving the pulse to a cell in a different state) leads to a bigger disturbance, some peak-to-peak distances close to 21h, others to 18h, and even if this is transitory, this might correspond to the type of data observed in the Group 2 of Table 1.

5. Alternative Hypotheses

5.1. Selective Activation of RevErb-α

The second solution found by the calibration procedure in section 4.2 is discussed here. The response curves for the period and phase are depicted in Fig. 10 and the corresponding values are summarized in Table 5.

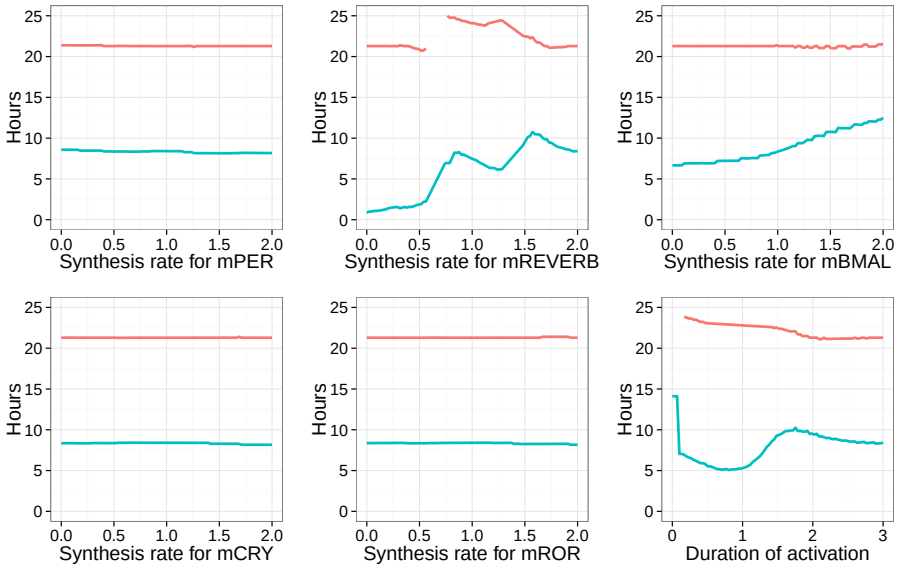

Figure 10: Period of the circadian clock (red) and phase between the division and RevErb-α (blue) in the coupled model calibrated with the second set of parameters, and when the cell cycle has a period of 21h.

kdie	FBS %	Circadian clock period (h)	Cell division period (h)	Phases (h)
0.077	5?	26.14	26.12	6.1
0.147	10	21.52	21.28	8.5
0.229	15	18.48	18.60	7.2

Table 5: Periods and time delays measured in the coupled model with different values of *kdie* for modeling the different culture conditions (the correspondance with 5% FBS is speculative since no experiment was done in this condition). The delays are the time observed by simulation between the peaks of concentration of MPF and RevErb-α.

For this solution similarly as for the first, the entrainment in period and phase of the circadian depends only on the effect of the mitosis on *Bmal1* and *RevErb-α*, and the duration of this effect. Varying the synthesis coefficients during mitosis for *Per*, *Cry* or *Ror* has no significant effect on the entrainment.

However in this case the entrainment in period depends on the effect on *RevErb-α*, which has to be activated with a coefficient close to 2 in order for the circadian clock to be entrained at 21h with a correct delay after division. Like in the previous case, an inhibition would also preserve the entrainment in period, but the phase would become inconsistent with the data. One can notice that an activation on *Bmal1* would also increase the time delay of RevErb-α peaks after division.

This solution points toward the activation of *RevErb-α* as an alternative hypothesis to explain the experimentally observed entrainment of the circadian clock in period and phase. Since RevErb-α is a repressor of *Bmal1* and Bmal1 an activator of *RevErb-α*, these two hypothesis correspond to two alternative mechanisms for a similar effect, and further experimental data would be needed to discriminate between them.

This hypothesis is modeled with a single activation of *RevErb-α* with a coefficient of 2 during mitosis, and no effect of mitosis on the other clock genes. This activation of *RevErb-α* might be caused by the transcription factor c-Myc which displays bursts of transcriptional activity during G1 phase (i.e., just after mitosis) and the S to G2/M transition of the cell cycle [26]. The c-Myc protein regulates its target genes through the same E-box DNA response element as the

Clock/Bmal1 heterodimer. It is therefore conceivable that during the G2/M phase of the cell cycle *RevErb-α* is positively regulated by c-Myc leading to the transcriptional repression of *Bmal1* as suggested by a recent study [27]. In this scenario the E-box regulated *Per* and *Cry* genes are expected to be also upregulated by the higher transcriptional activity of c-Myc. This is compatible with our simulations which show that the phase and period are resilient to variation of the coefficient synthesis for *Per* and *Cry*.

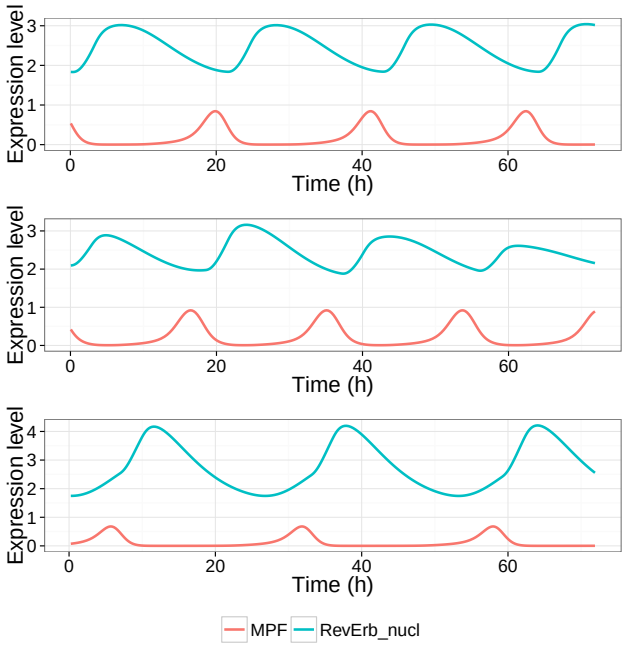

Figure 11: Simulation of the model with the activation of the transcription of *RevErb-α* triggered by mitosis, during 72h. Top: the cell cycle has a period of 21.3h. Middle: the cell cycle has a period of 20.1h. Bottom: : the cell cycle has a period of 26h.

Like the inhibition of *Bmal1* transcription, the activation of *RevErb-α* during 3h, triggered at mitosis, is able to entrain the circadian clock in a wide range of period (18-28h). Resulting traces are displayed in Fig. 11 for different cell cycle length conditions. However, the entrainment in phase, ie. the duration between mitosis and the following RevErb-α peak, differs between the two couplings, as seen in Fig: 12. In both cases, when the cell cycle has a period smaller than

24h, the circadian clock marker RevErb-α peaks 6h to 8h after mitosis. When the cell cycle period is greater than 24h, a notable difference can be seen for the predicted phase: with an activation of *RevErb-α*, RevErb-α still peaks just after the mitosis. But with an inhibition of *Bmal1*, RevErb-α peaks 18 to 24 fours after the mitosis. Although no experimental observations exist in a slowed down cell cycle condition, it is noteworthy that [8] and [13] report some cells dividing not long after the circadian peak where the circadian clock was found to be slowed down. This is the reason why we favor the hypothesis of *Bmal1* inhibition to the one of *RevErb-α* activation.

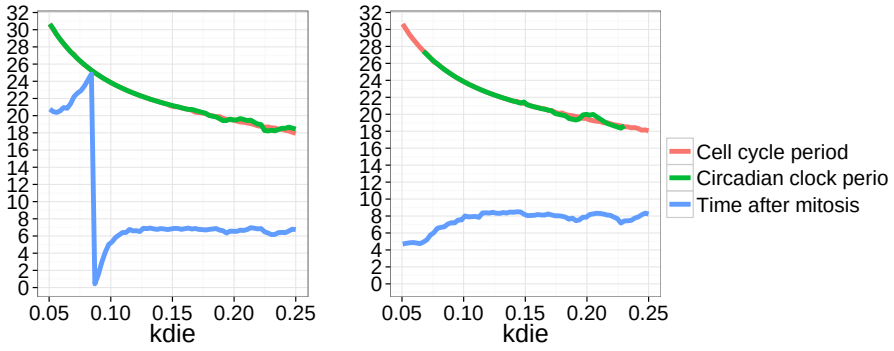

Figure 12: Entrainment in period and phase of the circadian clock when the period of the cell cycle varies with the parameter *kdie*, with the inhibition of *Bmal1* (left) or the activation of *RevErb-α* (right) triggered by mitosis. In the right panel, the circadian clock period is missing for low *kdie* values because the oscillations are irregular. The blue curves depict the time delay between peaks of MPF and RevErb-α in the simulations.

5.2. Uniform Inhibition of Transcription during Mitosis

It has been shown that in eukaryotes, gene transcription can be significantly inhibited during mitosis [17]. The impact of a global transcription inhibition of clock genes during mitosis on the circadian oscillator has been studied by modeling in [28]. In this study, the authors found that a periodic inhibition of transcription during one hour was able to entrain a model of the mammalian circadian clock, but only when the inhibition period was close to one half, twice or equal to the intrinsic circadian model period. In these cases, a phase locking between the circadian clock and the periodic inhibition was observed, albeit

with one or two preferential circadian phases for the inhibition and values that varied greatly with the inhibition period. The discrepancies with the recent data could come from the short inhibition duration considered or from the arbitrarily parameterised model used for the circadian clock, taken from [29].

In [1], we also investigated the uniform inhibition of all clock genes and found that it was sufficient to reproduce the entrainment of the circadian clock by the cell cycle in period, but not in phase. The delay between MPF and RevErb-α remained inconsistent with the data, as depicted in Fig. 13, i.e. the mitosis triggered by MPF occurs just after the peaks of RevErb-α, while the experimental studies consistently report the opposite: peaks of RevErb-α 5-7h after divisions. Furthermore, it seemed impossible to find parameter values to reproduce the observed delay under that hypothesis of a uniform inhibition of transcription during mitosis, which thus cannot explain the experimental data in mouse embryonic fibroblasts NIH3T3.

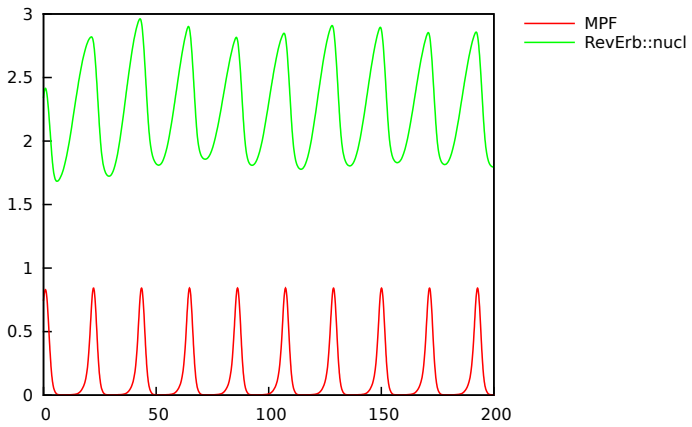

Figure 13: Entrainment to a period around 21.3h with $kampf = 3.75$ corresponding to a milieu enriched with 10% FBS, found in [1].

6. Conclusion

By hypothesizing a selective inhibition of *Bmal1* or a selective activation of *RevErb-α* triggered at the end of mitosis, we have been able to build a mechanis-

tic dynamical model which reproduces the somewhat surprising numerical data reported in [13, 14] about the acceleration of the circadian clock observed in dividing fibroblasts with high FBS concentrations. These observations suggest that the primary coupling between the cell division cycle and the circadian clock results from an influence of the cell cycle on the circadian clock in those cells. While considering a uniform inhibition of the transcription during mitosis [17] was shown to be sufficient to fit the period data in [1], the phase data reported in [14] seemed to be impossible to reproduce under that uniform inhibition hypothesis. The use of Biocham search algorithms for computing transcription inhibition parameters satisfying the phase observations formalized in quantitative temporal logic, led us to the hypothesis that at the end of mitosis, either the transcription of *Bmal1* has to be strongly inhibited, while no inhibition should affect the transcription of *RevErb-*α, or that *RevErb-*α has to be strongly activated. These two hypotheses differ by their predictions on slow cell cycle cells, possibly obtained with low levels of FBS, but for which no quantitative data are currently available.

Our model also postulates a different interpretation of some of the results presented in [14] when cells are treated by a 2h pulse of Dexamethasone. Instead of different autonomous cycling regimes, the model predicts temporary perturbations leading to shorter or longer peak-to-peak distances, but returning to the previous entrainment regime after some time, longer than the horizon used in the experiments.

Furthermore, in our coupled model, the phases between some of the clock gene products are shifted when entrained by a fast cell cycle. We are able to quantify these phase shifts and show that they concern mainly RevErb-α whose mRNA peaks are advanced by the periodic activation during mitosis. Other clock mRNAs and proteins are slightly delayed compared to their activator Bmal1. A prediction of the model is therefore that in quickly dividing cells, these protein peaks are shifted with respect to quiescent cells where such a phenomenon should not be observed.

On the other hand, our model leaves completely open the molecular mecha-

nisms responsible for the hypothesized selective inhibition of Bmal1, or activation of Reverb-α, at the end of mitosis and early G1. Several mechanisms can be imagined [30] and should be the matter of future experiments.

Acknowledgements.

This work has been partially funded by the ANR HyClock project (ANR-14-CE09-0011), ANR "Investments for the future" LABEX SIGNALIFE program (ANR-11-LABX-0028-01) and the former ERASysBio+ C5Sys project (ANR grant 2009-SYSB-002-02). This work was also granted access to the HPC resources of the CINES under the allocation c2015036437 made by GENCI.

[1] P. Traynard, F. Fages, S. Soliman, Model-based investigation of the effect of the cell cycle on the circadian clock through transcription inhibition during mitosis, in: O. Roux, J. Bourdon (Eds.), CMSB'15: Proceedings of the thirteenth international conference on Computational Methods in Systems Biology, Vol. 9308 of Lecture Notes in BioInformatics, Springer-Verlag, 2015, pp. 208–221. doi:10.1007/978-3-319-23401-4_18. URL http://lifeware.inria.fr/~fages/Papers/TFS15cmsb.pdf

[2] L. Glass, Synchronization and rhythmic processes in physiology, Nature 410 (6825) (2001) 277–84.

[3] T. Matsuo, S. Yamaguchi, S. Mitsui, A. Emi, F. Shimoda, H. Okamura, Control mechanism of the circadian clock for timing of cell division in vivo, Science 302 (5643) (2003) 255–259.

[4] J. W. Barnes, S. A. Tischkau, J. A. Barnes, J. W. Mitchell, P. W. Burgoon, J. R. Hickok, M. U. Gillette, Requirement of mammalian timeless for circadian rhythmicity, Science 302 (5644) (2003) 439–442.

[5] K. Ünsal-Kaçmaz, T. E. Mullen, W. K. Kaufmann, A. Sancar, Coupling of human circadian and cell cycles by the timeless protein, Molecular and Cellular Biology 25 (8) (2005) 3109–3116.

[6] A. Ballesta, S. Dulong, C. Abbara, B. Cohen, A. Okyar, J. Clairambault, F. Levi, A combined experimental and mathematical approach for molecular-based optimization of irinotecan circadian delivery, PLOS Computational Biology 7 (9).

[7] E. De Maria, F. Fages, A. Rizk, S. Soliman, Design, optimization, and predictions of a coupled model of the cell cycle, circadian clock, dna repair system, irinotecan metabolism and exposure control under temporal logic constraints, Theoretical Computer Science 412 (21) (2011) 2108–2127. doi:10.1016/j.tcs.2010.10.036.
URL http://lifeware.inria.fr/~fages/Papers/DFRS10TCS.pdf

[8] E. Nagoshi, C. Saini, C. Bauer, T. Laroche, F. Naef, U. Schibler, Circadian gene expression in individual fibroblasts: cell-autonomous and self-sustained oscillators pass time to daughter cells., Cell 119 (2004) 693–705.

[9] A. Gréchez-Cassiau, B. Rayet, F. Guillaumond, M. Teboul, , F. Delaunay, The circadian clock component bmal1 is a critical regulator of p21WAF1/CIP1 expression and hepatocyte proliferation, J Biol Chem 283 (2008) 4535–4542. doi:10.1074/jbc.M705576200.

[10] G. S1, K. N, B. L, Y. A, K. D, K. HP, The circadian gene per1 plays an important role in cell growth and dna damage control in human cancer cells, Mol Cell 22 (2006) 375–382.

[11] C. Gérard, A. Goldbeter, Entrainment of the mammalian cell cycle by the circadian clock: Modeling two coupled cellular rhythms, PLoS Comput Biol 8 (21) (2012) e1002516. doi:10.1371/journal.pcbi.1002516.

[12] L. Calzone, S. Soliman, Coupling the cell cycle and the circadian cycle, Research Report 5835, INRIA (Feb. 2006).
URL http://www.inria.fr/rrrt/rr-5835.html

[13] J. Bieler, R. Cannavo, K. Gustafson, C. Gobet, D. Gatfield, F. Naef, Robust synchronization of coupled circadian and cell cycle oscillators in single mammalian cells., Molecular systems biology 10 (7) (2014) 739.
URL http://www.ncbi.nlm.nih.gov/pubmed/25028488

[14] C. Feillet, P. Krusche, F. Tamanini, R. C. Janssens, M. J. Downey, P. Martin, M. Teboul, S. Saito, F. Lévi, T. Bretschneider, G. T. J. van der Horst, F. Delaunay, D. A. Rand, Phase locking and multiple oscillating attractors for the coupled mammalian clock and cell cycle., Proceedings of the National Academy of Sciences of the United States of America 111 (27) (2014) 9928–9833. doi:10.1073/pnas.1320474111.
URL http://www.pnas.org/content/111/27/9828.abstract

[15] A. Relógio, P. O. Westermark, T. Wallach, K. Schellenberg, A. Kramer, H. Herzel, Tuning the mammalian circadian clock: robust synergy of two loops., PLoS computational biology 7 (12) (2011) e1002309. doi:10.1371/journal.pcbi.1002309.
URL http://www.pubmedcentral.nih.gov/articlerender.fcgi?artid=3240597&tool=pmcentrez&rendertype=abstract

[16] Z. Qu, W. R. MacLellan, J. N. Weiss, Dynamics of the cell cycle: checkpoints, sizers, and timers, Biophysics Journal 85 (6) (2003) 3600–3611.

[17] D. Weisenberger, U. Scheer, A possible mechanism for the inhibition of ribosomal rna gene transcription during mitosis, Journal of Cell Biology.

[18] L. Calzone, F. Fages, S. Soliman, BIOCHAM: An environment for modeling biological systems and formalizing experimental knowledge, Bioinformatics 22 (14) (2006) 1805–1807. doi:10.1093/bioinformatics/btl172.
URL http://lifeware.inria.fr/~fages/Papers/bioinformatics.pdf

[19] F. Fages, P. Traynard, Temporal logic modeling of dynamical behaviors: First-order patterns and solvers, in: L. F. del Cerro, K. Inoue (Eds.),

Logical Modeling of Biological Systems, John Wiley & Sons, Inc., 2014, Ch. 8, pp. 291–323. doi:10.1002/9781119005223.ch8.
URL http://lifeware.inria.fr/~fages/Papers/FT14book.pdf

[20] P. Traynard, F. Fages, S. Soliman, Trace simplifications preserving temporal logic formulae with case study in a coupled model of the cell cycle and the circadian clock (best student paper award), in: CMSB'14: Proceedings of the twelth international conference on Computational Methods in Systems Biology, no. 8859 in Lecture Notes in BioInformatics, Springer-Verlag, 2014, pp. 114–128. doi:10.1007/978-3-319-12982-2.
URL http://lifeware.inria.fr/~fages/Papers/TFS14cmsb.pdf

[21] A. Rizk, G. Batt, F. Fages, S. Soliman, Continuous valuations of temporal logic specifications with applications to parameter optimization and robustness measures, Theoretical Computer Science 412 (26) (2011) 2827–2839. doi:10.1016/j.tcs.2010.05.008.
URL http://lifeware.inria.fr/~soliman/publi/RBFS11tcs.pdf

[22] A. Rizk, G. Batt, F. Fages, S. Soliman, A general computational method for robustness analysis with applications to synthetic gene networks, Bioinformatics 12 (25) (2009) il69–il78. doi:10.1093/bioinformatics/btp200.

[23] C. Feillet, G. T. J. van der Horst, F. Levi, D. A. Rand, F. Delaunay, Coupling between the circadian clock and cell cycle oscillators: Implication for healthy cells and malignant growth, Frontiers in Neurology 6 (May) (2015) 1–7. doi:10.3389/fneur.2015.00096.
URL http://www.frontiersin.org/Sleep{_}and{_}Chronobiology/10.3389/fneur.2015.00096/abstract

[24] F. Fages, A. Rizk, On temporal logic constraint solving for the analysis of

numerical data time series, Theoretical Computer Science 408 (1) (2008) 55–65. doi:doi:10.1016/j.tcs.2008.07.004.
URL http://lifeware.inria.fr/~fages/Papers/FR08tcs.pdf

[25] S. Yoo, S. Yamazaki, P. Lowrey, K. Shimomura, C. Ko, E. Buhr, S. Siepka, H. Hong, W. Oh, O. Yoo, M. Menaker, J. Takahashi, PERIOD2::LUCIFERASE real-time reporting of circadian dynamics reveals persistent circadian oscillations in mouse peripheral tissues, PNAS (2004) 5339–5346.

[26] A. Seth, S. Gupta, R. J. Davis, Cell cycle regulation of the c-Myc transcriptional activation domain, Molecular and cellular biology 13 (7) (1993) 4125–4136.

[27] B. J. Altman, A. L. Hsieh, A. Sengupta, S. Y. Krishnanaiah, Z. E. Stine, Z. E. Walton, A. M. Gouw, A. Venkataraman, B. Li, P. Goraksha-Hicks, et al., MYC disrupts the circadian clock and metabolism in cancer cells, Cell metabolism 22 (16) (2015) 1009–1019. doi:10.1016/j.cmet.2015.09.003.

[28] B. Kang, Y.-Y. Li, X. Chang, L. Liu, Y.-X. Li, Modeling the effects of cell cycle m-phase transcriptional inhibition on circadian oscillation, PLoS Comput Biol 4 (3) (2008) e1000019. doi:10.1371/journal.pcbi.1000019.
URL http://dx.plos.org/10.1371%2Fjournal.pcbi.1000019

[29] J.-C. Leloup, A. Goldbeter, Toward a detailed computational model for the mammalian circadian clock, Proceedings of the National Academy of Sciences 100 (2003) 7051–7056.

[30] P. Loyer, J. H. Trembley, R. Katona, V. J. Kidd, J. M. Lahti, Role of CDK/cyclin complexes in transcription and RNA splicing, Cellular Signalling 17 (9) (2005) 1033–1051. doi:10.1016/j.cellsig.2005.02.005.